Aromaticity in Semi-Condensed Figure-Eight Molecules

Albert Artigas, Yannick Carissan, Denis Hagebaum-Reignier, Harald Bock, Fabien Durola, Yoann Coquerel

Aromaticity in semi-condensed figure-eight molecules

Albert Artigas,[a] Yannick Carissan,[b] Denis Hagebaum-Reignier,[b] Harald Bock,[c] Fabien Durola,[c]* Yoann Coquerel[b]*

[a] Dr. A. Artigas, Facultat de Ciències, Universitat de Girona, Campus Montilivi, Carrer de Maria Aurèlia Capmany i Farnès 69, 17003 Girona, Catalunya, Spain
[b] Dr. Y. Carissan, Dr. D. Hagebaum-Reignier, Dr. Y. Coquerel, Aix Marseille Univ, CNRS, Centrale Méditerranée, iSm2, Marseille, France. E-mail: yoann.coquerel@univ-amu.fr
[c] Dr. H. Bock, Dr. F. Durola, Centre de Recherche Paul Pascal, CNRS, 115 av. Schweitzer, 33600 Pessac, France. E-mail: fabien.durola@crpp.cnrs.fr

Dedicated to Professor Miquel Solà on the occasion of his 60th birthday

Table of content graphic

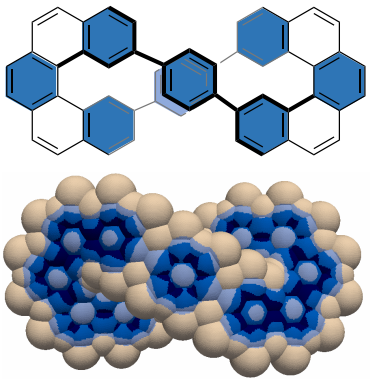

Aromaticity in the illustrated semi-condensed figure-eight molecule, a [5]helicene-bridged (1,4)cyclophane, is dominated by a (semi-)local character with some additional minor global character, as allowed by the small torsion angle along the single bonds.

Abstract

Electron delocalization and aromaticity was comparatively evaluated in recently synthesized figure-eight molecules made of two condensed U-shaped polycyclic aromatic hydrocarbon moieties connected either by two single bonds or by two para-phenylene groups. The selected examples include molecules that incorporate eight-membered and sixteen-membered rings, as well as a doubly [5]helicene-bridged (1,4)cyclophane. We probe whether some electron delocalization could occur through the stereogenic single bonds in these molecules: Is aromaticity purely (semi-)local, or possibly also global in these molecules? It was concluded that the situation can go from a purely (semi-)local character when the dihedral angle at the connecting single bonds is large, such as in biphenyl, to a predominantly (semi-)local character with a minor global contribution when the dihedral angle is small, such as in the para-phenylene connectors of the [5]helicene-bridged cyclophane.

Introduction

π-Conjugated macrocycles are molecules of enormous fundamental interest, but shape-persistent chiral π-conjugated macrocycles remain relatively rare.[1,2] Among these, lemniscate-shaped molecules, i.e. molecules that adopt the shape of the infinity symbol, also called figure-eight molecules, have recently attracted great attention. Amongst these, lemniscular porphyrinoids and related compounds of various sizes could be prepared and their properties examined,[3,4] and cyclo(hetero)arylene-based molecular lemnicates, in some cases with alkyne tethers, have also been investigated.[5] The field of π-conjugated figure-eight molecules has grown considerably in recent years because these molecules exhibit exciting chiroptical properties, especially circularly polarized luminescence.[6,7] Despite this, examples of fully condensed figure-eight polycyclic aromatic hydrocarbons (PAH) made only of six-membered rings are extremely scarce because the synthesis of such molecules remains a formidable challenge: two successful syntheses of *twisted carbon nanobelts* embedding anthracene subunits were reported,[8] and the synthesis of an all-ortho fused molecule, known as *infinitene*, was also achieved.[9] Aromaticity is an old chemical concept, yet the topic of considerable interest and controversy.[10] When analyzing electron delocalization and aromaticity in these fully condensed figure-eight molecules, it was found that their main aromatic character can go from local (ring currents are restricted to a single six-membered ring) with well-localized Clar π-sextets in the *twisted carbon nanobelts*[8], to global (ring currents cover the entire system) with macrocyclic electron delocalization in *infinitene*.[11] It seems that the main factor inducing or inhibiting a global aromatic character in these molecules is the connectivity of the six-membered rings, i.e., the existence or not of anthracene subunits. Another class of valuable figure-eight π-conjugated compounds are macrocyclic dimers in which two U-shaped condensed aromatic moieties are connected by single bonds. It was previously demonstrated that the presence of C(sp^2)–C(sp^2) single bonds is not an obstacle to global aromaticity when the torsion angle between the phenyl rings is moderate. For instance, [7]cycloparaphenylene exhibits a weak macrocyclic global aromatic ring current, with a strength of ca. 25% of the ring current strength in benzene, albeit the torsion angles between some of its phenyl rings are up to 28°.[12] In the cases of figure-eight molecules made of U-shaped condensed aromatic moieties connected by single bonds, we wondered: How does the presence of the single bonds affect the macrocyclic aromatic properties in these molecules? Herein, we attempt to answer this question through the analysis of electron delocalization and aromaticity in four selected representative cases using visual methods that allow for straightforward qualitative comparisons.

Computational methods based on magnetic criteria are extremely useful for the assessment of aromaticity.[13] The physical principle underlying these tools is the application of an external magnetic field to a molecule and calculating its magnetic response. The externally applied magnetic field should be normal to the π system to obtain the most meaningful results. While there is no ambiguity about the normal to the π system for planar compounds, i.e., perpendicular to the molecular plane, the situation is more complex for twisted and 3D π-conjugated molecules such as figure-eight molecules. In these cases, it may be preferable to use isotropic approaches averaging the magnetic response in the three directions of space. Among these, isovalue plots of the anisotropy of the magnetically induced current densities (ACID)[13c] and isocontour plots of isotropic magnetic shielding

(IMS) are valuable indicators of the magnetically induced current densities.[14] As a complementary electronic criterion of aromaticity, isovalue plots of the electron density of delocalized bonds, $EDDB_H(r)$,[15] have also been used for this study.

Results and discussion

We selected four exemplary macrocycles for analysis, three of which are dimers in which two condensed monomeric units are directly linked by two single bonds to form a macrocycle: As the prototype of a lemniscular PAH, cyclobisphenanthrene, or dibenzo[*def*,*pqr*]tetraphenylene (**1**, Figure 1a), was first synthesized by Thulin and Wennerström through a two-fold transannular Mallory cyclization,[16] and more recently by Murakami, Itami and co-workers by a palladium-catalyzed cyclodimerization of 4-chloro-phenanthrene.[17] A π-extended and maximally sextet-stabilized derivative of **1**, cyclobistriphenylene, or dinaphtho[1,2,3,4-*def*:1',2',3',4'-*pqr*]tetraphenylene (**2**, Figure 1b), was first prepared by Ramakrishna and Sharp through the dimerization of a nickelacyle[18] and more recently by Murakami, Itami and co-workers by a palladium-catalyzed cyclodimerization of 1-chlorotriphenylene.[17] As a differently shaped figure-eight, cyclobis[5]helicene **3** (Figure 1c) was first synthesized by Thulin and Wennerström through an iterative two-fold transannular Mallory cyclization,[19] and an octaester-substituted analog was more recently reported through a modified approach.[20] All three macrocycles **1**, **2** and **3** are very rigid with a barrier to enantiomerization computed higher than 200 $kJ{\cdot}mol^{-1}$.[6] The torsion angles between the six-membered rings connected by the stereogenic single bonds are 75° (±14°) in **1**, 80° (±13°) in **2**, and 63° (±4°) in **3**, indicating no unusual strain around these single bonds. In comparison, the torsion angle in biphenyl is 44°.[21] Electron delocalization and aromaticity in figure-eight molecules **1**–**3** have not been examined previously.

The ACID isosurface of **1** was generated together with the ACID isosurface of phenanthrene for comparison (Figure 1a). These ACID plots show a strong predominance at the edges of all phenanthrene subunits, indicating the existence of relatively important ring current circuits there, even though the macrocyclic ring current density at the edges is possibly exaggerated as an inherent drawback of the method.[22] The existence of a global macrocyclic ring current circuit at the edge of phenanthrene is not in contradiction with the co-existence of other local current circuits, for instance in the two terminal six-membered rings of each phenanthrene unit,[23] in agreement with its Clar structure. To determine whether the magnetically induced current densities in the figure-eight molecule **1** flow either diatropically to correspond to an aromatic character, or paratropically to correspond to an antiaromatic character, one could perform a magnetically induced current density analysis[13d] to visualize the current densities as vectors plotted onto the ACID isosurface. However, the result of this analysis heavily depends on the orientation of the applied external magnetic field, which can produce significantly different outputs (see Figure S1 in the Supporting Information for an illustration of this). The 3D IMS contour maps of phenanthrene and **1** only show neutral or blue color indicating positive values of IMS corresponding to an aromatic character of both molecules. On the 3D IMS contour map of **1**, the local circuit in the terminal six-membered rings of the phenanthrene subunits are well visualized (dark blue color), as well as the less intense semi-local (i.e. encompassing more

than one six-membered ring) ring current circuits at the phenanthrene subunits edges (medium blue color). Satisfactorily, the differences between the two magnetically non-equivalent faces of each ring are also clearly visualized. It is noticeable that IMS around the two single bonds[24] connecting the phenanthrene units in **1** is small as visualized by the essentially neutral color indicating negligible delocalization there. In agreement with this, the $EDDB_H(r)$ calculations provided two strictly disconnected isosurfaces on both sides of the two single bonds connecting the phenanthrene units in **1**. Comparable observations can be made about the ACID isosurfaces, 3D IMS contour maps, and $EBBD_H(r)$ isosurfaces of triphenylene and macrocycle **2** (Figure 1b). Altogether, these analyses of aromaticity in figure-eight molecules **1** and **2** suggest that they are both composed of two independent twisted chiral phenanthrene-type and triphenylene-type aromatic systems, respectively, showing (semi-)local aromaticity.

As for macrocycles **1** and **2**, the ACID analyses of [5]helicene itself and macrocyle **3** (Figure 1c) show a predominance at the edges of each [5]helicene unit, and mostly blue-colored 3D IMS maps pointing to a diatropic magnetically induced current. In the 3D IMS map of **3**, close inspection revealed some tiny areas of light blue color on the surface around the single bonds connecting both [5]helicene units. This is just a threshold effect: the maximum IMS determined on the surface over the single bonds in **1** and **2** is around 5.0 ppm (corresponding to neutral color), while the maximum IMS is around 6.0 ppm (corresponding to light blue) over the single bonds in **3**. These positive IMS values may not be attributed to the existence of π-type effects but more as reference values for σ-type effects. Complementary $EDDB_H(r)$ calculations confirmed that two strictly disconnected isosurfaces exist on both sides of the two single bonds connecting the [5]helicene units. These analyses suggest that the two aromatic [5]helicene units in **3** are independent with only (semi-)local aromaticity. This is consistent with the photophysical properties of an octaester-substituted analog of **3**, which showed that it behaves essentially as a dimer of the corresponding [5]helicene tetraester.[20]

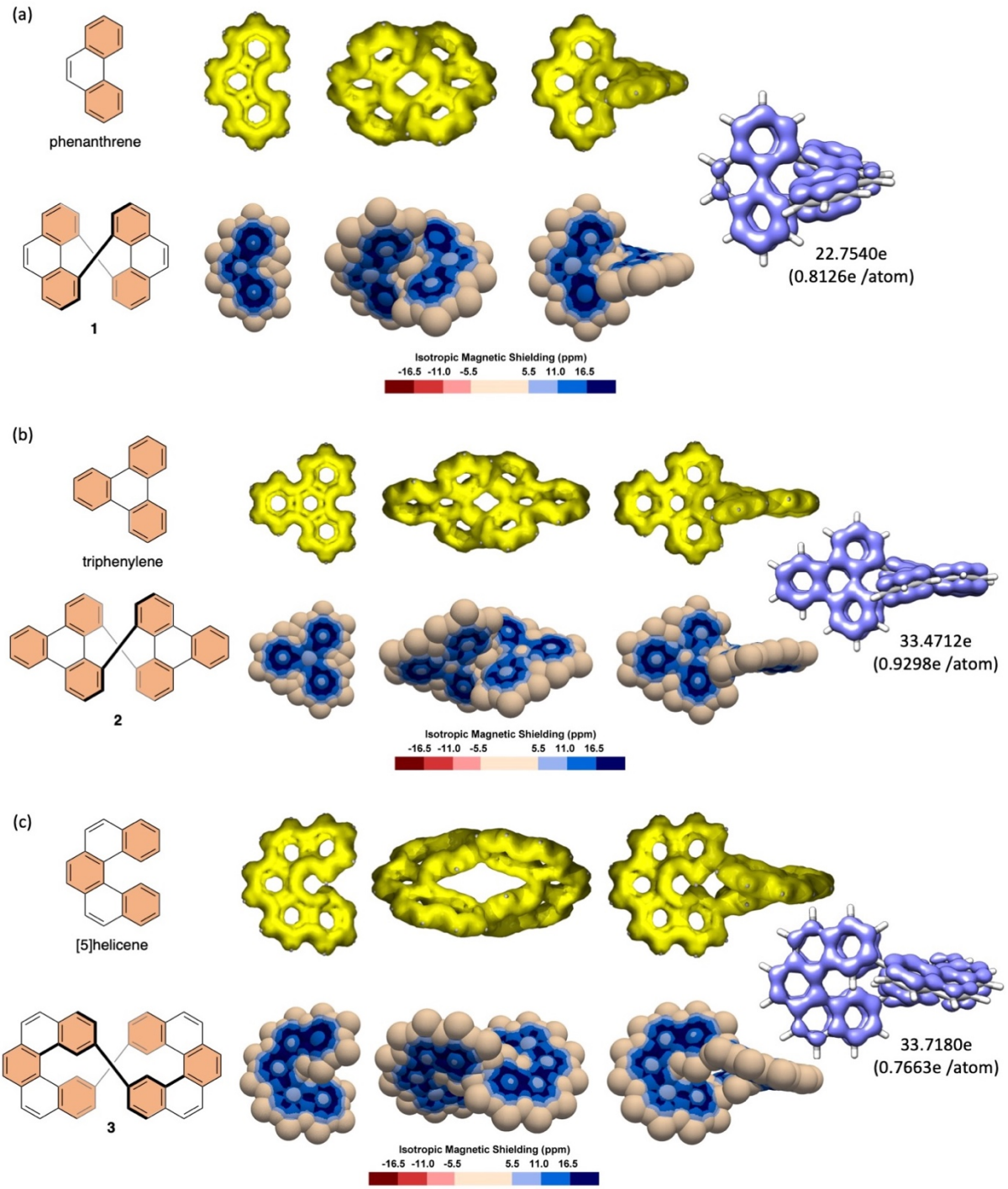

Figure 1. Visualization of electron delocalization and aromaticity in (a) phenanthrene and cyclobisphenanthrene **1**, (b) triphenylene and cyclobistriphenylene (**2**), (c) [5]helicene and cyclobis[5]helicene **3**, using Clar structures with π-sextets localized in the colored rings, ACID isosurfaces (yellow, isovalue = 0.03), 3D IMS isocontour maps, and $EDDB_H(r)$ isosurfaces (blue, isovalue = 0.02) together with $EDDB_H(r)$ quantitative values.

In 2020, Hirose, Matsuda and co-workers reported the synthesis and photophysical properties of the doubly [5]helicene-bridged (1,4)cyclophane **4** (Figure 2) as an alternative shape-persistent figure-eight dimer of [5]helicene.[25] The photophysical properties of macrocycle **4** differ significantly from the ones of **3**: the UV-vis absorption maximum of **4** is considerably red-shifted with respect to **3** ($\lambda_{max,abs}$ = 390 nm for **4** in chloroform[25], $\lambda_{max,abs}$ = 241 and 284 nm for **3** in cyclohexane[19]), and the luminescence dissymmetry factor $|g_{lum}|$ of **4** was determined at 0.015, which is in the upper range of values for organic molecules and a three-fold enhancement when compared to the $|g_{lum}|$ determined for the octaester-substituted analog of **3**.[6] These data illustrate the differences in the ground and excited electronic states of macrocycles **3** and **4**, including their chiral nature. A careful examination of the crystal structure of **4** obtained by single-crystal X-ray diffraction[25] revealed that, in the solid state, macrocycle **4** is not D_2-symmetric as presumed, but C_2-symmetric, with the two central phenylene rings not coplanar to each other, and with unequal torsion angles with the two attached [5]helicenyl moieties: ca. 3° (±1°) on one side and 25° (±1°) on the other side. Our own DFT calculations of the optimized geometry of **4** in the gas phase were consistent with the solid-state structural experimental data and indicated that the most stable conformation of **4** is C_2-symmetric. The D_2-symmetric geometry of **4** with coplanar phenylene rings stacked could be identified computationally, but as a transition state with relative $\Delta G^{\ddagger}$ = 2.8 kJ·mol^{-1} (P = 1 atm, T = 298.15 K, freq #1 = -39.7 cm^{-1}), corresponding to the synchronized rotation of these rings around the single bonds. Considering the tiny $\Delta G^{\ddagger}$ rotation barrier, corresponding to $t^{1/2}_{rotation}$ < 1 ps at 25 °C, the time-averaged structure of **4** has the D_2-symmetric geometry of its transition state with the two phenylene rings coplanar and 10° (±1°) torsion angles at the C(sp^2)–C(sp^2) single bonds.

Aromaticity in D_2-**4** was very recently examined using a π-only approach and it was concluded that no global aromaticity exists in **4**,[26] with four independent, not conjugated π-type systems coexisting in D_2-**4**: two [5]helicene systems and two benzene systems. In the ACID analysis of both C_2-**4** and D_2-**4**, all edges of the [5]helicene and central benzene moieties are strongly expressed indicating semi-local current circuits there. The 3D IMS contour map of C_2-**4** and D_2-**4** deserve a closer look. The IMS patterns over the [5]helicenyl units of both geometries are comparable with the one in [5]helicene itself and with the one in **3**, with somehow overall reduced intensity. The two [5]helicene moieties in C_2-**4** are visibly not magnetically equivalent. Considering the central para-phenylene rings, their IMS patterns in C_2-**4** show continuous circular dark blue areas that can be compared with the one in benzene itself.[14] In contrast, the IMS patterns over of the two central benzene rings in D_2-**4** show discontinuous dark blue areas. This is certainly a consequence of the different geometries and the different spatial alignment of these two rings with the rest of the structure. It could be verified through the analysis of artificially stacked benzene dimers that it is not a consequence of through-space ring-to-ring magnetization.[2j] The IMS patterns of the two central phenyl rings in D_2-**4** resembles the patterns obtained previously for an analogous triply [5]helicene-bridged (1,3,5)cyclophane.[2j] The most striking difference between the 3D IMS maps of macrocycles **1**–**3** and macrocycle **4** is the continuous light blue color on both faces of the surface around the four single bonds linking the two central para-phenylene rings with the two [5]helicene units in **4**. Maximum IMS on the surface around the single bonds in C_2-**4** was measured at 7.9–8.4 ppm on the convex face and at 9.2–9.4 ppm on the concave face, and at 9.0 ppm (convex face) and 10.0 ppm (concave face) for D_2-**4**. The different values of IMS on both faces reflect the torsion of the molecule, with a better

overlap of *p*-type orbitals on the concave faces. For D_2-**4**, the maximum IMS value around the single bonds is nearly the double of the value found for **3** and it is more comparable with the value found in *s-cis*-butadiene (11.0 ppm[14]), a π-conjugated diene. This suggest that beyond σ-type-only effects, additional π-type effects of small magnitude are present. Accordingly, for the central para-phenylene rings in **4**, the absolute values of NICS(±1) are decreasing from C_2-**4** (-8.3 ppm on the convex face, and -9.9 ppm on the concave face), to D_2-**4** (-7.3 ppm on the convex face, and -9.1 ppm on the concave face). Comparatively, the value for benzene at the same level of theory is -10.2 ppm. The $EDDB_H(r)$ analyses of both C_2-**4** and D_2-**4** are consistent with their 3D IMS analyses, both qualitatively and quantitatively. Quantitatively, the slightly greater value of $EDDB_H(r)$ in D_2-**4** compared to C_2-**4** is consistent with more global delocalization in D_2-**4** than in C_2-**4**. Qualitatively, considering the central para-phenylene rings, discontinuous isosurfaces are observed on the convex faces and continuous isosurfaces are observed on the concave faces in both geometries. At the convex faces of C_2-**4** and D_2-**4**, one can perceive the influence of the different torsion angles along the single bonds by evaluating the gap between the isosurfaces: when the torsion angle is ca. 3–10° as in D_2-**4** and on one side of C_2-**4**, the isosurfaces are very close one to another with a tiny gap, when the torsion angle is ca. 25° as on the other side of C_2-**4**, the isosurfaces are more distant.

The complementary investigations conducted here with the all-electron approach led to a different conclusion to the π-only approach, indicating that the π-type systems of D_2-**4** are not fully independent. A consequence of torsion in π-conjugated molecules is that, strictly speaking, pure σ and π systems no longer exist as they overlap (and overlap differently on the convex and concave faces): σ and π electronic systems are approximations in the case of contorted molecules. Thus, computational analysis of aromaticity –a property of the π system for organic molecules– in contorted PAHs, especially helicene-containing molecules,[27] is not straightforward. It can be done either using the π-only approach through the use of artificial methods to approximate a pure π system,[28,29] or using the all-electron approach while trying to minimize the contributions from the core and σ-type electrons. Both approaches are inaccurate: in the π-only approach the bias comes from the definition of the π system itself, and in the all-electron approach the main bias originates for the contribution of the σ-type system.

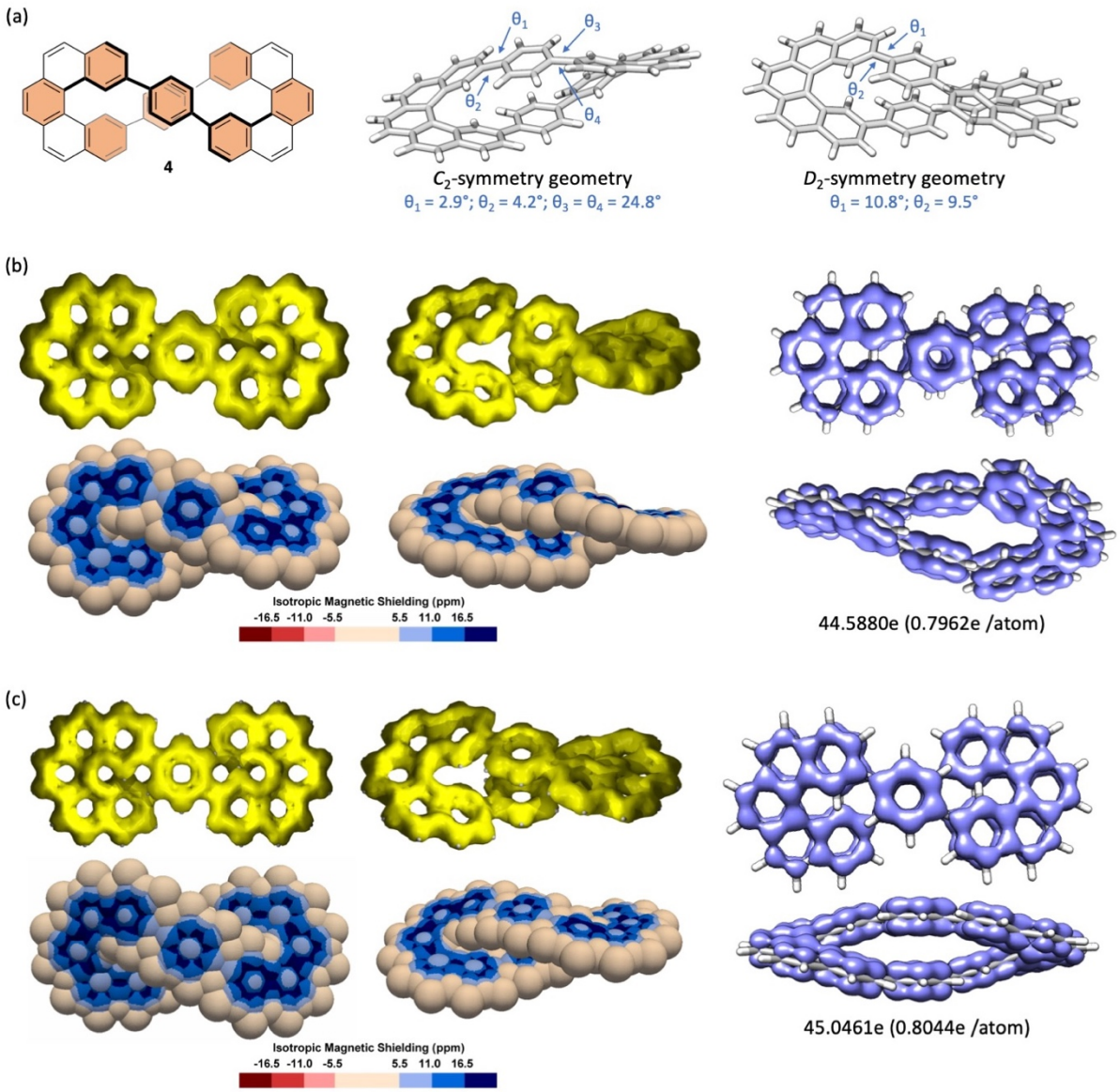

Figure 2. (a) Lewis representation and geometries of doubly [5]helicene-bridged (1,4)cyclophane **4**. Visualization of electron delocalization and aromaticity in (b) C_2-**4** and (c) D_2-**4** using ACID isosurface (yellow, isovalue = 0.03), 3D IMS contour maps, and $EDDB_H(r)$ isosurfaces (blue, isovalue = 0.02) together with $EDDB_H(r)$ quantitative values.

Conclusion

Electron delocalization and aromaticity was examined in four representative figure-eight molecules in which two U-shaped condensed polycyclic aromatic hydrocarbon moieties are connected by single bonds or by para-phenylene bridges. Analyses were conducted using the all-electron approach through isotropic magnetic criteria and electronic criteria of aromaticity. It could be concluded that cyclobisphenanthrene **1**, cyclobistriphenylene **2**, and cyclobis[5]helicene **3** exhibit purely (semi-)local aromaticity with no π-type conjugation through the stereogenic single bonds connecting the two condensed polycyclic aromatic units. The main reasons for this are geometrical: all three molecules are very rigid with torsion angles at the single bonds exceeding 60°, which preclude π-type ring-to-ring delocalization. In contrast, the doubly [5]helicene-bridged (1,4)cyclophane **4** is a more flexible molecular architecture and in its time-averaged D_2-symmetric geometry the torsion angle at the single bonds is 10°, now rendering possible π-type ring-to-ring delocalization. Recent examination of the aromaticity in **4** using the π-only approach led to the conclusion that such π-type ring-to-ring delocalization does not exist, with four strictly independent π-type electron systems in **4**.[26] Our own complementary analysis conducted with the all-electron approach suggests that some weak π-type ring-to-ring delocalization over the single bonds occurs in **4**, which is corroborated by the optical characteristics of **4**. Overall, aromaticity in **4** seems to be dominated by a (semi-)local character, with a minor but significant additional global character. This situation is apparently comparable to that of the triply [5]helicene-bridged (1,3,5)cyclophane that we recently synthesized and analyzed,[2j] for which the existence of a minor global aromatic character was evidenced by all-electron analysis. This study is one more illustration of the complexity in assessing aromaticity in conjugated but not fully condensed macrocyclic π-conjugated organic compounds.

Computational methods

All geometries were optimized with the Gaussian 16 package.[30] The geometries of molecules **1**, **2** and **3** were optimized using the B3LYP hybrid density functional[31] with the D3BJ correction for dispersion[32] and the def2-SVP basis set[33] without symmetry constraints. The geometries of C_2-**4** and D_2-**4** were optimized using the BP86 density functional[34] with the D3BJ correction for dispersion and the def2-SVP basis set. Analytical Hessians were computed to confirm that the optimized geometries are indeed minima (zero imaginary frequency) or transition states (one imaginary frequency).

From the optimized geometries, ACID calculations were performed using the B3LYP/6-31+G(d,p) level of theory.[13c] The continuous set of gauge transformation (CSGT) method was used to calculate current densities,[35] as implemented in the Gaussian 16 package. The ACID scalar field represents the density of delocalized electrons and is visualized by an isosurface (in yellow).

For the 3D IMS contour maps, pseudo-van der Waals surfaces of *Bq* made of overlapping spheres of 1 Å radius centered on the nuclei (and some additional selected positions) were generated using a purpose-built code.[14] NMR-GIAO calculations[36] at every *Bq* were performed at the B3LYP-GIAO/6-311++G(d,p)[37] level and using the CPHF(Separate)

keyword to improve accuracy. The 3D IMS contour maps are interactive and are available for visualization (and personalization) in the Supporting Information as .vtk files. Single point NICS(±1) values were read directly from the 3D IMS maps.

EDDB(r) isosurfaces[15] were computed at the CAM-B3LYP/6-311G(d,p)[38] level of theory using NBO 6.0 software first to obtain the natural atomic orbitals and then running the EDDB program available at www.aromaticity.eu. The EDDB(r) isosurfaces were generated using the Formchk and Cubegen tools implemented in the Gaussian 16 package. Paraview visualization software was used to visualize 3D IMS maps and generate the corresponding pictures. Molecular graphics and analyses were performed with UCSF Chimera.[39]

Acknowledgments
This work was funded by the French Agence Nationale de la Recherche − ANR (ANR-13-JS07-0009, ANR-19-CE07-0041, ANR-20-CE07-0014). A.A. acknowledges the Spanish Ministerio de Universidades and the EU for a Margarita Salas grant (REQ2021_A_02). Institutional financial support from Aix-Marseille University, Centrale Méditerranée, the Centre Régional de Compétences en Modélisation Moléculaire, the University of Bordeaux, and the CNRS is acknowledged.

Data availability statement
The data that support the findings of this study are available in the supplementary material of this article.

Conflict of interest
The authors declare no conflict of interest.

Keywords
aromaticity • chirality • hydrocarbons • helicene • cyclophane

Author contribution
YCo and FD conceived the study and performed funding acquisition. AA, YCa, DHR and YCo performed calculations. All authors performed data analysis and contributed to the final manuscript.

References

[1] Reviews: a) M. Stępień, N. Sprutta, L. Latos-Grażyński, *Angew. Chem. Int. Ed.* **2011**, *50*, 4288. b) M. Rickhaus, M. Mayor, M. Juríček, *Chem. Soc. Rev.* **2016**, *45*, 1542. c) M. Rickhaus, M. Mayor, M. Juríček, *Chem. Soc. Rev.* **2017**, *46*, 1643. d) M. A. Majewski, M. Stępień, *Angew. Chem. Int. Ed.* **2019**, *58*, 86.

[2] a) G. Naulet, L. Sturm, A. Robert, P. Dechambenoit, F. Röhricht, R. Herges, H. Bock, F. Durola, *Chem. Sci.* **2018**, *9*, 8930. b) R. Kurosaki, M. Suzuki, H. Hayashi, M. Fujiki, N. Aratani, H. Yamada, *Chem. Commun.* **2019**, *55*, 9618. c) E. Kayahara, T. Iwamoto, H. Takaya, T. Suzuki, M. Fujitsuka, T. Majima, N. Yasuda, N. Matsuyama, S. Seki, S. Yamago, *Nat. Commun.* **2013**, *4*, 2694. d) K. Matsui, Y. Segawa, T. Namikawa, K. Kamada, K. Itami, *Chem. Sci.* **2012**, *4*, 84. e) J. Zhu, Y. Han, Y. Ni, S. Wu, Q. Zhang, T.

Jiao, Z. Li, J. Wu, *J. Am. Chem. Soc.* **2021**, *143*, 14314. f) A. Basavarajappa, M. D. Ambhore, V. G. Anand, *Chem. Commun.* **2021**, *57*, 4299. g) N. Hayase, J. Nogami, Y. Shibata, K. Tanaka, *Angew. Chem. Int. Ed.* **2019**, *58*, 9439. h) Y. Ni, F. Gordillo-Gámez, M. Peña Alvarez, Z. Nan, Z. Li, S. Wu, Y. Han, J. Casado, J. Wu, *J. Am. Chem. Soc.* **2020**, *142*, 12730. i) T. Matsushima, S. Kikkawa, I. Azumaya, S. Watanabe, *ChemistryOpen* **2018**, *7*, 278. j) F. Aribot, A. Merle, P. Dechambenoit, H. Bock, A. Artigas, N. Vanthuyne, Y. Carissan, D. Hagebaum-Reignier, Y. Coquerel, F. Durola, *Angew. Chem. Int. Ed.* **2023**, *62*, e202304058. k) S. Hitosugi, W. Nakanishi, T. Yamasaki, H. Isobe, *Nat. Commun.* **2011**, *2*, 492. l) P. Sarkar, Z. Sun, T. Tokuhira, M. Kotani, S. Sato, H. Isobe, *ACS Cent. Sci.* **2016**, *2*, 740. m) G. Naulet, A. Robert, P. Dechambenoit, H. Bock, F. Durola, *Eur. J. Org. Chem.* **2018**, 619. n) L. Zhu, W. Zeng, M. Li, M. Lin, *Chinese Chem. Lett.* **2022**, *33*, 229.

[3] Reviews: a) M. Stępień, N. Sprutta, L. Latos-Grażyński, *Angew. Chem. Int. Ed.* **2011**, *50*, 4288. b) B. Szyszko, M. J. Białek, E. Pacholska-Dudziak, L. Latos-Grażyński, *Chem. Rev.* **2017**, *117*, 2839.

[4] Recent work: a) K. C. Sahoo, M. A. Majewski, M. Stępień, H. Rath, *J. Org. Chem.* **2017**, *82*, 8317. b) I. Casademont-Reig, T. Woller, J. Contreras-García, M. Alonso, M. Torrent-Sucarrat, E. Matito, *Phys. Chem. Chem. Phys.* **2018**, *20*, 2787. c) Z. Liu, T. Lu, S. Hua, Y. Yu, *J. Phys. Chem. C* **2019**, *123*, 18593. d) A. Ghosh, S. Dash, A. Srinivasan, C. H. Suresh, S. Peruncheralathan, T. K. Chandrashekar, *Org. Chem. Front.* **2019**, *6*, 3746. e) M. Rickhaus, M. Jirasek, L. Tejerina, H. Gotfredsen, M. D. Peeks, R. Haver, H.-W. Jiang, T. D. W. Claridge, H. L. Anderson, *Nat. Chem.* **2020**, *12*, 236. f) C. Li, Z. Huang, Y. Hu, W. Liang, R. Su, M. Chen, L. Zhou, D. Wu, G. Gao, J. You, Org. Lett. **2021**, *23*, 3746. g) K. Wypych, M. Dimitrova, D. Sundholm, M. Pawlicki, *Org. Lett.* **2022**, *24*, 4876. h) B. Yadav, M. Ravikanth, *J. Org. Chem.* **2022**, *87*, 2543. i) H. S. Udaya, A. Basavarajappa, T. Y. Gopalakrishna, V. G. Anand, *Chem. Commun.* **2022**, *58*, 13931. j) Q. Wang, J. Pyykkö, M. Dimitrova, S. Taubert, D. Sundholm *Phys. Chem. Chem. Phys.* **2023**, *25*, 12469.

[5] a) H. Nie, Q.-H. Li, S. Zhang, C.-M. Wang, W.-H. Lin, K. Deng, L.-J. Shu, Q.-D. Zeng, J.-H. Wan *Org. Chem. Front.* **2021**, *8*, 6806. b) L. H. Wang, N. Hayase, H. Sugiyama, J. Nogami, H. Uekusa, K. Tanaka, *Angew. Chem. Int. Ed.* **2020**, *59*, 17951. c) S. M. Bachrach, *J. Org. Chem.* **2020**, *85*, 674. d) T. A. Schaub, E. A. Prantl, J. Kohn, M. Bursch, C. R. Marshall, E. J. Leonhardt, T. C. Lovell, L. N. Zakharov, C. K. Brozek, S. R. Waldvogel, S. Grimme, R. Jasti, *J. Am. Chem. Soc.* **2020**, *142*, 8763. e) Z. Zhang, W.-Y. Cha, N. J. Williams, E. L. Rush, M. Ishida, V. M. Lynch, D. Kim, J. L. Sessler, *J. Am. Chem. Soc.* **2014**, *136*, 7591. f) L.-H. Wang, J. Nogami, Y. Nagashima, K. Tanaka, *Org. Lett.* **2023**, *25*, 4225. g) Z. Luo, X. Yang, K. Cai, X. Fu, D. Zhang, Y. Ma, D. Zhao, *Angew. Chem. Int. Ed.* **2020**, *59*, 14854. h) G. R. Kiel, K. L. Bay, A. E. Samkian, N. J. Schuster, J. B. Lin, R. C. Handford, C. Nuckolls, K. N. Houk, T. D. Tilley, *J. Am. Chem. Soc.* **2020**, *142*, 11084. i) J. Wang, Y.-Y. Ju, K.-H. Low, Y.-Z. Tan, J. Liu, *Angew. Chem. Int. Ed.* **2021**, *60*, 11814.

[6] A. Robert, G. Naulet, H. Bock, N. Vanthuyne, M. Jean, M. Giorgi, Y. Carissan, C. Aroulanda, A. Scalabre, E. Pouget, F. Durola, Y. Coquerel, *Chem. Eur. J.* **2019**, *25*, 14364.

[7] a) A. Ushiyama, S. Hiroto, J. Yuasa, T. Kawai, H. Shinokubo, *Org. Chem. Front.* **2017**, *4*, 664. b) K. Senthilkumar, M. Kondratowicz, T. Lis, P. J. Chmielewski, J. Cybińska, J. L. Zafra, J. Casado, T. Vives, J. Crassous, L. Favereau, M. Stępień, *J. Am. Chem. Soc.* **2019**, *141*, 7421. c) Y. Nojima, M. Hasegawa, N. Hara, Y. Imai, Y. Mazaki, *Chem. Eur. J.* **2021**, *27*, 5923. d) L. Zhan, H. Xiao, J.-N. Gao, H. Cong, *Org. Chem. Front.* **2023**, *10*, 5395. e) T.

Honda, D. Ogata, M. Tsurui, S. Yoshida, S. Sato, T. Muraoka, Y. Kitagawa, Y. Hasegawa, J. Yuasa, H. Oguri, *Angew. Chem. Int. Ed.* **2024**, e202318548.

[8] a) W. Fan, T. Matsuno, Y. Han, X. Wang, Q. Zhou, H. Isobe, J. Wu, *J. Am. Chem. Soc.* **2021**, *143*, 15924. b) Q. Zhou, X. Hou, J. Wang, Y. Ni, W. Fan, Z. Li, X. Wei, K. Li, W. Yuan, Z. Xu, M. Zhu, Y. Zhao, Z. Sun, J. Wu, *Angew. Chem. Int. Ed.* **2023**, *62*, e202302266.

[9] M. Krzeszewski, H. Ito, K. Itami *J. Am. Chem. Soc.* **2022**, *144*, 862.

[10] a) P. v. R. Schleyer, *Chem. Rev.* **2001**, *101*, 1115. b) A. Stanger, *Chem. Commun.* **2009**, 1939. c) N. Martín, L. T. Scott, *Chem. Soc. Rev.* **2015**, *44*, 6397. d) G. Merino, M. Solà, *Phys. Chem. Chem. Phys.* **2016**, *18*, 11587. e) M. Solà, *Front. Chem.* **2017**, *5*, 22. f) M. Solà, *Nature Chem.* **2022**, *14*, 585. g) M. Solà, A. I. Boldyrev, M. K. Cyrański, T. M. Krygowski, G. Merino, Aromaticity and Antiaromaticity: Basics and Applications, John Wiley & Sons, Inc., Hoboken, **2023**. h) G. Merino, M. Solà, I. Fernández, C. Foroutan-Nejad, P. Lazzeretti, G. Frenking, H. L. Anderson, D. Sundholm, F. P. Cossío, M. A. Petrukhina, J. Wu, J. I. Wu, A. Restrepo, *Chem. Sci.* **2023**, *14*, 5569. i) H. Ottoson, *Chem. Sci.* **2023**, *14*, 5542. j) M. Solà, I. Fernández, G. Merino, *Chem. Sci.* **2023**, *14*, 9628.

[11] M. Orozco-Ic, R. R. Valiev, D. Sundholm, *Phys. Chem. Chem. Phys.* **2022**, *24*, 6404.

[12] S. Taubert, D. Sundholm, F. Pichierri, *J. Org. Chem.* **2010**, *75*, 5867.

[13] a) R. Islas, T. Heine, G. Merino, *Acc. Chem. Res.* **2012**, *45*, 215. b) R. Gershoni-Poranne, A. Stanger, *Chem. Soc. Rev.* **2015**, *44*, 6597. c) D. Geuenich, K. Hess, F. Köhler, R. Herges, *Chem. Rev.* **2005**, *105*, 3758. d) D. Sundholm, H. Fliegl, R. J. F. Berger, *Wiley Interdiscip. Rev.: Comput. Mol. Sci.* **2016**, *6*, 639. e) A. Stanger, *Eur. J. Org. Chem.* **2020**, 3120.

[14] A. Artigas, D. Hagebaum-Reignier, Y. Carissan, Y. Coquerel, *Chem. Sci.* **2021**, *12*, 13092.

[15] a) D. W. Szczepanik, M. Andrzejak, J. Dominikowska, B. Pawelek, T. M. Krygowski, G. Szatylowicz, M. Solà, *Phys. Chem. Chem. Phys.* **2017**, *19*, 28970. b) D. W. Szczepanik, M. Solà in *Aromaticity: Modern Computational Methods and Applications*, Ed.: I. Fernández, Elsevier, **2021**, Chap. 8, pp. 259-283.

[16] B. Thulin, O. Wennerström, *Tetrahedron Lett.* **1977**, *18*, 929.

[17] S. Matsubara, Y. Koga, Y. Segawa, K. Murakami, K. Itami, *Nat. Catal.* **2020**, *3*, 710.

[18] T. V. V. Ramakrishna, P. R. Sharp, *Organometallics* **2004**, *23*, 3079.

[19] a) B. Thulin, O. Wennerström, *Acta Chem. Scand. Sect. B* **1976**, *30*, 688. b) E. M. Kosower, H. Dodiuk, B. Thulin, O. Wennerström, *Acta Chem. Scand. Sect. B* **1977**, *31*, 526.

[20] B. A. Robert, P. Dechambenoit, E. A. Hillard, H. Bock, F. Durola, *Chem. Commun.* **2017**, *53*, 11540.

[21] a) A. Almenningen, O. Bastiansen, L. Fernholt, B. N. Cyvin, S. J. Cyvin, S. Samdal, *J. Mol. Struct.* **1985**, *128*, 59. b) M. P. Johansson, J. Olsen, *J. Chem. Theory Comput.* **2008**, *4*, 1460.

[22] A. Soncini, P. W. Fowler, L. W. Jenneskens, *Phys. Chem. Chem. Phys.* **2004**, *6*, 277.

[23] L. Leyva-Parra, R. Pino-Rios, D. Inostroza, M. Solà, M. Alonso, W. Tiznado, *Chem. Eur. J.* **2023**, e202302415.

[24] a) P. B. Karadakov, K. E. Horner, *J. Phys. Chem. A* **2013**, *117*, 518. b) P. B. Karadakov, K. E. Horner, *J. Chem. Theory Comput.* **2016**, *12*, 558. c) B. J. Lampkin, P. B. Karadakov, B. VanVeller, *Angew. Chem. Int. Ed.* **2020**, *59*, 19275. d) P. B. Karadakov, B. Vanveller, *Chem. Commun.* **2021**, *57*, 9504.

[25] H. Kubo, D. Shimizu, T. Hirose, K. Matsuda, *Org. Lett.* **2020**, *22*, 9276.
[26] M. Orozco-Ic, L. Soriano-Agueda, S. Escayola, D. Sundholm, G. Merino, E Matito *J. Org. Chem.* **2024**, https://doi.org/10.1021/acs.joc.3c02485
[27] a) G. Portella, J. Poater, J. M. Bofill, P. Alemany, M. Solà, *J. Org. Chem.* **2005**, *70*, 2509. b) M. Orozco-Ic, J. Barroso, N. D. Charistos, A. Muñoz-Castro, G. Merino, *Chem. Eur. J.* **2020**, *26*, 326.
[28] a) P. W. Fowler, E. Steiner, *Chem. Phys. Lett.* **2002**, *364*, 259. b) M. Antić, S. Đorđević, B. Furtula, S. Radenković, *J. Phys. Chem. A* **2020**, *124*, 371. c) M. Orozco-Ic, M. Dimitrova, J. Barroso, D. Sundholm, G. Merino, *J. Phys. Chem. A* **2020**, *125*, 5753.
[29] A. Stanger, *J. Org. Chem.* **2010**, *75*, 2281.
[30] Gaussian 16, Revision A.03, M. J. Frisch, G. W. Trucks, H. B. Schlegel, G. E. Scuseria, M. A. Robb, J. R. Cheeseman, G. Scalmani, V. Barone, G. A. Petersson, H. Nakatsuji, X. Li, M. Caricato, A. V. Marenich, J. Bloino, B. G. Janesko, R. Gomperts, B. Mennucci, H. P. Hratchian, J. V. Ortiz, A. F. Izmaylov, J. L. Sonnenberg, D. Williams-Young, F. Ding, F. Lipparini, F. Egidi, J. Goings, B. Peng, A. Petrone, T. Henderson, D. Ranasinghe, V. G. Zakrzewski, J. Gao, N. Rega, G. Zheng, W. Liang, M. Hada, M. Ehara, K. Toyota, R. Fukuda, J. Hasegawa, M. Ishida, T. Nakajima, Y. Honda, O. Kitao, H. Nakai, T. Vreven, K. Throssell, J. A. Montgomery, Jr., J. E. Peralta, F. Ogliaro, M. J. Bearpark, J. J. Heyd, E. N. Brothers, K. N. Kudin, V. N. Staroverov, T. A. Keith, R. Kobayashi, J. Normand, K. Raghavachari, A. P. Rendell, J. C. Burant, S. S. Iyengar, J. Tomasi, M. Cossi, J. M. Millam, M. Klene, C. Adamo, R. Cammi, J. W. Ochterski, R. L. Martin, K. Morokuma, O. Farkas, J. B. Foresman, and D. J. Fox, Gaussian, Inc., Wallingford CT, 2016.
[31] a) D. E. Woon, T. H. Dunning, *J. Chem. Phys.*, **1993**, *98*, 1358. b) C. Lee, W. Yang, R. G. Parr, *Phys. Rev. B*, **1988**, *37*, 785.
[32] S. Grimme, J. Antony, S. Ehrlich, H. Krieg, *J. Chem. Phys.* **2010**, *132*, 154104.
[33] F. Weigend, R. Ahlrichs, *Phys. Chem. Chem. Phys.* **2005**, *7*, 3297–3305.
[34] J. P. Perdew, *Phys. Rev. B* **1986**, *33*, 8822.
[35] T. A. Keith, R. F. W. Bader, *J. Chem. Phys.* **1993**, *99*, 3669.
[36] K. Wolinski, J. F. Hinton, P. Pulay, *J. Am. Chem. Soc.* **1990**, *112*, 8251.
[37] M. J. Frisch, J. A. Pople, J. S. Binkley, *J. Chem. Phys.* **1984**, *80*, 3265.
[38] T. Yanai, D. P. Tew, N. C. Handy, *Chem. Phys. Lett.* **2004**, *393*, 51.
[39] E. F. Pettersen, T. D. Goddard, C. C. Huang, G. S. Couch, D. M. Greenblatt,E. C. Meng, T. E. Ferrin, *J. Comput. Chem.* **2004**, *25*, 1605.